

Title

Hydrolytic Metabolism of Cyanopyrrolidine DPP-4 Inhibitors Mediated by Dipeptidyl

Peptidases

Fandi Kong, Xiaoyan Pang, Jihui Zhao, Pan Deng, Mingyue Zheng, Dafang Zhong, Xiaoyan Chen.

Shanghai Institute of Materia Medica, Chinese Academy of Sciences, Shanghai 201203, China (F.K., X.P., P. D., D.Z., M.Z., X.C.)

University of Chinese Academy of Sciences, Beijing 100049, China (F.K., D.Z., M.Z., X.C.)

School of Life Science and Technology, Shanghai Tech University, Shanghai 201210, China (J.Z.)

Running Title: Hydrolytic Metabolism of Cyanopyrrolidine DPP-4 Inhibitors

Corresponding Author:

Xiaoyan Chen

Shanghai Institute of Materia Medica, Chinese Academy of Sciences, 501 Haik Road, Shanghai,
201203, China;

Phone: +86-21-50800738; Fax: 0086-21-50800738;

Email: xychen@sim.ac.cn

Number of text pages: 31

Number of tables: 0

Number of figures: 12

Number of references: 16

Number of words in the Abstract: 250

Number of words in the Introduction: 475

Number of words in the Discussion: 1498

Abbreviations: anagliptin-COOH: the carboxylic acid metabolite of anagliptin; BCA: Bicinchoninic acid; besigliptin-COOH: the carboxylic acid metabolite of besigliptin; CN: nitrile; DASH: DPP-4 activity and/or structure homologue; DPP: dipeptidyl peptidase; FAP: fibroblast activation protein- α ; HPLC: high-performance liquid chromatography; SD rats: Sprague–Dawley rats; vildagliptin-COOH: the carboxylic acid metabolite of vildagliptin;

Abstract

Nitrile group biotransformation is an unusual or minor metabolic pathway for most nitrile-containing drugs. However, for some cyanopyrrolidine dipeptidyl peptidase-4 (DPP-4) inhibitors (vildagliptin, anagliptin, and besigliptin, not saxagliptin), the conversion of nitrile group into carboxylic acid is their major metabolic pathway *in vivo*. DPP-4 was reported to be partly involved in the metabolism. In our pilot study, it was also observed that saxagliptin, a DPP-4 specific inhibitor, decreased the plasma exposures of besigliptin carboxylic acid in rats by only 20%. Therefore, it is speculated that some other enzymes may participate in nitrile group hydrolysis. After incubating gliptins with the cytosol, microsomes, and mitochondria of liver and kidney, carboxylic acid metabolites could all be formed. In recombinant DPP family such as DPP-4, DPP-2, DPP-8, DPP-9, and fibroblast activation protein- α , more hydrolytic metabolites were found. Among them, DPP-2 had the highest hydrolytic capacity besides DPP-4. And DPP-4 inhibitor saxagliptin and DPP-2 inhibitor AX8819 can both inhibit the hydrolysis of gliptins. Western blot results showed that DPP-2 and DPP-4 existed in the above subcellular organelles at varying amounts. In rats, AX8819 decreased the plasma exposures of besigliptin carboxylic acid by 40%. The amide intermediates of gliptins were detected *in vivo* and *in vitro*. When the amide derivatives of gliptins were incubated with DPP-4, they were completely hydrolyzed at a rate far more than that from the parent drug, including saxagliptin-amide. Therefore, it was proposed that gliptins, except saxagliptin, were initially hydrolyzed to their amides by DPPs, which was the rate-limiting step in generating the carboxylic end-product.

Introduction

The nitrile (CN) group is introduced as an efficacious pharmacophore into the increasing number of therapeutic drugs. It can enhance the selectivity and binding affinity of these drugs to target proteins via hydrogen bond, covalent, polar, and π - π interactions. Moreover, nitrile is introduced to block metabolically labile sites because nitrile biotransformation is rather rare and, when observed, is a minor metabolic pathway (Fleming et al., 2010). However, the nitrile group is not stable as it was expected for cyanopyrrolidine dipeptidyl peptidase-4 (DPP-4) inhibitors, namely, vildagliptin (He et al., 2009a) (Novartis, Switzerland), anagliptin (Furuta et al., 2013) (Sanwa Kagaku Kenkyusho Co., Ltd., Japan), and besigliptin (Jiangsu Hansoh Pharmaceutical Co., Ltd., China, under clinical phases) (Fig. 1). The hydrolysis of the nitrile group to a carboxyl group is their major metabolic pathway *in vivo*. However, there is an obvious exception to this; the nitrile group of saxagliptin (a cyanopyrrolidine DPP-4 inhibitor on the market, Bristol-Myers Squibb, USA) cannot be hydrolyzed (Su et al., 2012).

It has been reported that DPP-4 could mediate the CN hydrolysis of vildagliptin (He et al., 2009a; Asakura et al., 2015) and anagliptin (Furuta et al., 2013). However, in DPP-4-knockout rats, the formation of vildagliptin carboxylic acid metabolite (vildagliptin-COOH) was only decreased by approximately 20%. Therefore, it is speculated that some other enzymes may participate in CN hydrolysis. DPP-4 (EC 3.4.14.5), also known as CD26, is a serine peptidase that cleaves off N-terminal dipeptides containing proline, hydroxyproline, or alanine at the penultimate position, such as glucagon-like peptide-1 and glucose-dependent insulintropic polypeptide (Gautier et al., 2005). DPP-4 activity and/or structure homologue (DASH) proteins include some other DPPs, such as DPP-

2, DPP-8, DPP-9, and fibroblast activation protein- α (FAP). They all belong to the serine peptidase family with a common catalytic triad of Ser, Asp, and His residues in sequence and share similar substrate specificity (Matteucci and Giampietro, 2009), indicating that they might also have the potential hydrolysis ability of the nitrile group. Some severe side effects caused by DPP-4 inhibitors, such as anemia, thrombocytopenia, splenomegaly, lymphadenopathy, lung histiocytosis, mortality with multiple organ pathology, and gastrointestinal and central nervous system toxicity, were reported to be the probable result of the nonspecific inhibition of DPP-8 and DPP-9 (Matteucci and Giampietro, 2009). Thus, to avoid off-target effects in the development of DPP-4 inhibitors, DPP-2, DPP-8, DPP-9, and FAP are often selected for screening specific DPP-4 inhibitors. In the present study, the roles of other dipeptidyl peptidases except DPP-4 were investigated during CN hydrolysis metabolism of gliptins. Moreover, the possible mechanism of why saxagliptin could not be hydrolyzed was also discussed.

Besigliptin was employed as a model drug to conduct *in vivo* pharmacokinetic experiments in rats and combined with vildagliptin, anagliptin, and saxagliptin to investigate the enzymes involved in the hydrolysis of the nitrile group. Besigliptin is a cyanopyrrolidine DPP-4 inhibitor that is in clinical development. Its main metabolite in humans is also the carboxylic acid metabolite (besigliptin-COOH) hydrolyzed from the nitrile group. The plasma exposure of besigliptin-COOH was about eightfold of the parent drug after an oral dose of besigliptin in humans (unpublished data).

Materials and methods

Chemicals and reagents. Besigliptin, its carboxylic acid metabolite, and its amide derivative were all kindly provided by Jiangsu Hansoh Pharmaceutical Co., Ltd. (Lianyungang, China). Saxagliptin and vildagliptin were purchased from Meilun Biology Technology Co., Ltd. (Dalian, China). Anagliptin was obtained from Chengdu Novel Biochemical Technology Co., Ltd. (Chengdu, China). Amide derivatives of saxagliptin and vildagliptin were purchased from Phystandard Bio-Tech Co., Ltd. (Shenzhen, China). AX8819 was synthesized as previously described (Danilova et al., 2007). Tris was purchased from Sangon Biotech Co., Ltd. (Shanghai, China). Bicinchoninic acid (BCA) protein assay kit was obtained from Beyotime (Shanghai, China). Human liver homogenate, cytosol, mitochondria, microsomes, and kidney homogenate were purchased from BD Gentest (Woburn, MA, USA). Recombinant DPP-4 and DPP-2 were obtained from GenScript Corporation (Nanjing, China). DPP-8, DPP-9, and FAP were kindly provided by Dr. Jingya Li in the National Center for Drug Screening, Shanghai, China. All solvents for LC-MS/MS analysis were of high-performance liquid chromatography (HPLC) grade (Merck, Darmstadt, Germany). Other reagents were of analytical grade.

Isolation of rat hepatic and renal subcellular organelles. Male Sprague–Dawley (SD) rats weighing 180–220 g were sacrificed via exsanguination of the abdominal aorta under anesthesia, and the livers or kidneys were promptly removed. One portion of rat liver or kidney sample was homogenized with the five-fold volume of ice-cold phosphate buffer (250 mM sucrose, 10 mM Tris-HCl, 1 mM EDTA-2Na, pH 7.4) before centrifuging at 600 g for 10 min at 4°C to remove tissue debris and nuclei. The supernatant was spun at 9000 g for 20 min to obtain the S9 fraction. The

resulting pellet comprised mitochondria and was washed once before analysis. The S9 fraction was further centrifuged at 100 000 *g* for 60 min at 4°C to separate the cytosolic and microsomes components. Each pellet was dissolved in adequate homogenization buffer and stored at –80°C. The protein content was determined using the BCA protein assay kit.

Subcellular organelle incubations. Besigliptin (0.25 μM), vildagliptin (0.50 μM), and anagliptin (0.50 μM) were respectively incubated with different organelles (protein concentration: 4 mg/mL) at 37°C for 3 h, including microsomes, mitochondria, and cytosol of rat liver, rat kidney, and human liver. The hydrolysis was also investigated in homogenates (protein concentration: 4 mg/mL) of the liver and kidney in rats and humans. The incubation system comprised phosphate-buffered saline (PBS, 100 mM, pH 7.5) with 0.5 mM MgCl₂. The time and protein concentration had been investigated in a pre-study to avoid saturation. The total volume was 200 μL. Reactions were terminated with an equal volume of ice-cold acetonitrile. Samples were stored at –80°C until LC-MS/MS analysis.

Immunoblot analysis of kidney and liver homogenate and their subcellular organelles. The liver homogenate, mitochondria, microsomes, and cytosol were diluted to the desired protein concentration with 4X Lithium dodecyl sulfate buffer after the measurement of protein concentrations using BCA protein assay kit. Samples were separated by 4%–20% Bis-Tris polyacrylamide gel electrophoresis (GenScript, Nanjing, Jiangsu, China) and transferred to a PVDF membrane. Blots were probed with the primary antibody of 1: 100 dilution of rabbit anti-DPP-2 polyclonal antibody (Thermo Fisher Scientific, Cambridge, MA, USA; PA5-54369) and 1: 1000 dilution of rabbit anti-DPP-4 monoclonal antibody (Abcam, Cambridge, MA, USA; ab28340). β-

actin (1: 500 dilution) (Santa Cruz Biotechnology, Dallas, TX, USA; sc-517576) was selected as the loading control for homogenates. No proper endogenous protein was evenly distributed in the cytosol, mitochondria, and microsomes. Thus, the same loading amounts were roughly ensured by loading the same amount of proteins measured through the BCA method. The signal was visualized by adding chemiluminescent agent (Millipore, Billerica, MA, USA) after incubating with a 1: 2000 dilution of the secondary horseradish peroxidase-labeled antibody (goat anti-rabbit IgG) (KPL, Gaithersburg, MD, USA; 04-15-06).

Hydrolysis of gliptins and amide derivatives in recombinant DPPs. Besigliptin, vildagliptin, anagliptin, saxagliptin, and their amide derivatives, except anagliptin (terminal concentration: 100 μ M), were respectively incubated with DPP-4, DPP-2, DPP-8, DPP-9, and FAP in PBS with their optimum pH (DPP-4: pH 7.5; DPP-2: pH 5.5; DPP-8/9 and FAP: pH 8.0) at 37°C for 3 h. The concentration of DPPs was set at the same hydrolytic activity of serine according to the National Center for Drug Screening (Shanghai, China). Each treatment was performed in duplicate.

To compare the reaction rate of gliptin as substrate with amide derivative as substrate, besigliptin (100 μ M) and its amide (100 μ M) were separately incubated at 37°C in the recombinant DPP-4 (5.00 μ g/mL) incubation system at designated time points.

The reaction rates from three gliptin amide derivatives to the corresponding carboxylic acid metabolites were further compared. Amide derivatives (50.0 μ M) of besigliptin, vildagliptin, and saxagliptin were separately incubated with DPP-4 (5.00 μ g/mL) at 37°C and designated time points to investigate the rate of carboxylic acid formation.

Reactions were terminated with an equal volume of ice-cold acetonitrile. Samples were stored at

–80°C until UPLC/Triple TOF 5600⁺ MS Analysis.

Inhibition of nitrile group hydrolysis in recombinant DPP-4 and DPP-2. To verify the involvement of DPP-2 and DPP-4 in the hydrolysis of gliptins, besigliptin (10.0 μM), vildagliptin (10.0 μM), and anagliptin (10.0 μM) were separately incubated with recombinant DPP-4 (5.00 μg/mL) and DPP-2 (5.00 μg/mL) at 37°C for 3 h in the presence or absence of DPP-4 inhibitor, saxagliptin (50.0 μM), or DPP-2 inhibitor, AX8819 (50.0 μM). Reactions were terminated with an equal volume of ice-cold acetonitrile. Samples were stored at –80°C until LC-MS/MS analysis.

Animal experiments. All procedures involving animals were performed in accordance with the *Guide for the Care and Use of Laboratory Animals* of the Shanghai Institute of Materia Medica, Chinese Academy of Sciences. The animals were fasted for 12 h with free access to water before the experiments. Male SD rats weighing 180–220 g were acclimatized for at least seven days before the experiments.

To investigate the effects of saxagliptin (DPP-4 inhibitor) on besigliptin metabolism, rats were randomly divided into control and saxagliptin-treated groups. The saxagliptin-treated rats were orally administered with 100 mg/kg/day saxagliptin formulated in 0.5% sodium carboxymethyl cellulose (CMC-Na) for four successive days, and the control group of rats was orally administered with the corresponding vehicle control. At 15 min after the last dose, the two groups of rats were orally administered with 3 mg/kg besigliptin dissolved in 0.5% CMC-Na. Blood samples were collected at 10, 20, and 40 min, as well as 1.0, 1.5, 2.0, 3.0, 5.0, 7.0, and 10 h after besigliptin dosage in tubes containing an anticoagulant (EDTA-2K) and 100 μM saxagliptin (to avoid further hydrolysis of besigliptin by DPP-4 in the blood). Plasma samples were centrifuged at 11 000 *rpm* for 5 min at 4°C

and then stored at -80°C until analysis.

The effects of AX8819 (DPP-2 inhibitor) on besigliptin metabolism were evaluated using the method above. The dosage of AX8819 was 50 mg/kg, whereas the dosage of besigliptin was 1 mg/kg.

Sample pretreatment. The samples from rat pharmacokinetic study were prepared as follows. A 25.0 μL aliquot plasma sample and 25.0 μL of internal standard (15.0 ng/mL SHR116022) were mixed with 150 μL of acetonitrile. After the samples were vortexed and centrifugated at 14 000 *rpm* for 5 min, the supernatants were used to measure besigliptin and its carboxylic acid with LC-MS/MS analysis.

The samples from subcellular organelle incubation experiments and inhibition experiments on DPP-2 and DPP-4 were pretreated as follows. A 50.0 μL aliquot of samples and 25.0 μL of internal standard (15.0 ng/mL SHR116022) were mixed with 125 μL of acetonitrile. After vortexing and centrifugation at 14 000 *rpm* for 5 min, the supernatants were used to measure gliptins and their carboxylic acid by LC-MS/MS method.

Samples from the hydrolysis experiments of gliptins and amide derivatives in recombinant DPPs for verification of the mechanism of hydrolysis were vortexed for 1 min and centrifuged at 14 000 *rpm* and 4°C for 5 min. The supernatants were evaporated to dryness at 40°C in a nitrogen stream and then reconstituted in 100 μL of water/methanol (90: 10, v/v). A 10.0 μL aliquot of the reconstituted solution was injected into the UPLC/Triple TOF 5600+ system for analysis.

UPLC/Triple TOF 5600⁺ MS Analysis. Metabolite identification was performed using an Acquity UPLC system (Waters Corp, Milford, MA, USA) and a Triple TOF 5600⁺ system (Applied

Biosystems, Ontario, Canada). Chromatographic separation was achieved on UPLC HSS T3 (100 mm × 2.1 mm id, 1.8 μ m; Waters) at 40°C. The mobile phase was a mixture of 5 mM ammonium acetate containing 0.1% formic acid (A) and acetonitrile (B) at a flow rate of 0.400 mL/min. The gradient elution program began from 1% B and maintained for 1 min, then increased linearly to 99% B in the next 15 min, and maintained for 1 min; in the next 0.5 min, the gradient was reduced to 1% B linearly and maintained at 1% B until the gradient was stopped at 20 min.

MS detection was performed on a Triple TOF 5600⁺ mass spectrometer. The mass range was set at *m/z* 50–1000, and the other parameters were set as follows: ion spray voltage, 5500 V; declustering potential, 80 V; ion source heater, 550°C; curtain gas, 35 psi; ion source gas 1, 60 psi; and ion source gas 2, 60 psi. For TOF MS scans, the collision energy was 10 eV; for product scans, the collision energy was 25 eV, and the collision energy spread was 15 eV. Information-dependent acquisition, together with real-time multiple mass defect filter, was used to trigger the acquisition of MS/MS spectra. The compounds were detected in positive electrospray ionization (ESI⁺) mode. The extracted ions were 384.2411 (besigliptin-amide), 385.2251 (besigliptin-COOH), 322.2131 (vildagliptin-amide), 323.1971 (vildagliptin-COOH), 402.2254 (anagliptin-amide), 403.2094 (anagliptin-COOH), 335.1971 (saxagliptin-amide), and 334.2131 (saxagliptin-COOH).

LC-MS/MS analysis. The parent drugs and their carboxylic acid metabolites were determined on a Shimadzu LC-30AD HPLC system (Kyoto, Japan) tandem with an API 5500 triple-quadrupole MS (Applied Biosystems, Ontario, Canada). The Analyst 1.6.3 software (Applied Biosystems) was used for data acquisition and processing. The mobile phase was a mixture of 5 mM ammonium acetate containing 0.1% formic acid (A) and acetonitrile (B).

The chromatographic separation of besigliptin and its carboxylic acid metabolite was achieved on Venusil ASB-C18 (50 mm × 4.6 mm id, 5 μm; Angela Technologies Inc., Newark, DE, USA) at 40°C. The mobile phase was set at A and B (6: 4, v/v) at a flow rate of 0.65 mL/min. Multiple reaction monitoring (m/z 366 → 195 for besigliptin, m/z 385 → 195 for besigliptin-COOH, m/z 334 → 165 for SHR116022 as internal standard) was used in the ESI+ mode with an ion spray voltage of 4500 V and a source temperature of 500°C. The nebulizer gas, heater gas, and curtain gas were set to 50, 50, and 20 psi, respectively. The standard curve ranges ranged from 1 nM to 1000 nM.

Chromatographic separation of vildagliptin and its carboxylic acid metabolite was achieved on a HILIC (100 mm × 3.0 mm id, 3 μm; Phenomenex, Inc., Torrance, CA, USA) at 40°C. The flow rate was 0.80 mL/min. The gradient elution program began from 90% B and maintained for 0.8 min, then decreased linearly to 75% B in the next 0.5 min, and maintained for 0.9 min; in the next 0.1 min, the gradient was increased to 90% B linearly and maintained until the gradient was stopped at 4.2 min. Multiple reaction monitoring (m/z 304 → 154 for vildagliptin, m/z 323 → 116 for vildagliptin-COOH, m/z 334 → 165 for SHR116022 as internal standard) was used in the ESI+ mode. Other conditions were the same as above.

Chromatographic separation of anagliptin and its carboxylic acid metabolite was achieved on UPLC HSS T3 (50 mm × 2.1 mm id, 1.8 μm; Waters) at 40°C. The flow was 0.50 mL/min. The gradient elution program began from 90% B and maintained for 0.5 min, then decreased linearly to 80% B in the next 0.5 min, and maintained for 0.5 min; in the next 0.5 min, the gradient was increased to 90% B linearly and maintained until the gradient was stopped at 4.0 min. Multiple reaction monitoring (m/z 384 → 231 for anagliptin and m/z 403 → 231 for anagliptin-COOH) was

used in the ESI+ mode. Other conditions were the same as above.

Data analysis. Data are presented as the mean \pm standard deviation ($n \geq 3$) or mean of duplicate.

WinNonlin (version 6.1, Pharsight Corp, Cary, NC, USA) was used to calculate the pharmacokinetic parameters in a non-compartmental model. Student's two-tailed unpaired t -test in SPSS (version 20.0, SPSS Inc., Chicago, IL, USA) was used to determine the difference. The level of statistical significance was set at $p < 0.05$.

Results

Identification of besigliptin carboxylic acid and amide metabolites in human plasma and urine samples. Figs. 2A and 2B show the metabolic profiles in human plasma sample (2 h post-dose) and urine sample (0–24 h) after an oral dose of 100 mg besigliptin, respectively. M2 was a major metabolite in both plasma and urine samples with a protonated molecule at m/z 385.225, which has an identical chromatographic behavior and product ions with the besigliptin-COOH standard. The typical ion spectra of M2 (besigliptin-COOH) are shown in Supplemental Fig. S1B. Trace amount of M8-2 was detected in the human urine sample with a protonated molecule at m/z 384.241, which has the same chromatographic retention and product ions with besigliptin-amide standard (Supplemental Fig. S1C).

Hydrolysis of gliptins in liver and kidney subcellular organelles. Besigliptin, vildagliptin, and anagliptin were hydrolyzed to their corresponding carboxylic acid metabolites in rat and human liver, kidney, and plasma. In addition, the production of carboxylic acid metabolites was in descending order in the hepatic mitochondria, microsomes, and cytosol (Fig. 3). Because it was difficult to obtain human kidney subcellular organelles, only rat kidney organelles were used to investigate the hydrolysis. Carboxylic acid metabolites of besigliptin, vildagliptin, and anagliptin were also produced in the mitochondria, microsomes, and cytosol of rat kidney in descending order (Fig. 3).

Hydrolysis of gliptins in recombinant DPPs. The hydrolysis of four gliptins was investigated in DPPs, including DPP-4, DPP-2, DPP-8, DPP-9, and FAP (Fig. 4). Except saxagliptin, the carboxylic acid metabolites of three gliptins were detected in all DPP-included systems (Figs. 4A–4C). Among them, the DPP-2 incubation system generated the most carboxylic acid metabolites, and DPP-9

formed the least. Saxagliptin could not be hydrolyzed in any DPP (Fig. 4D). Additionally, the amide metabolites of gliptins were detected in all of the incubation system, including the buffer of pH 5.5 and pH 8.0. Moreover, the amount of amide metabolites formed in alkaline buffer was larger than that formed in acidic buffer. In the buffer with pH 5.5, the produced amide metabolites in the buffer alone were less than those in the buffer with DPP-2, indicating the DPPs (DPP-2 in particular) were involved in the formation of amide metabolites.

Inhibition of gliptin hydrolysis in recombinant DPP-4 and DPP-2. The effect of selective inhibitors (saxagliptin and AX8819) on the production of carboxylic acid metabolites was investigated. In recombinant human DPP-4, besigliptin, vildagliptin, and anagliptin were hydrolyzed to their carboxylic acid metabolites (Figs. 5A, 5C, and 5E). Saxagliptin almost entirely inhibited the hydrolysis of gliptins, up to 84.6% for besigliptin, 93.5% for vildagliptin, and 96.0% for anagliptin, but AX8819 did not.

Recombinant human DPP-2 was also able to hydrolyze besigliptin, vildagliptin, and anagliptin to their carboxylic acid metabolites, and the hydrolysis was inhibited by AX8819 up to 91.7% for besigliptin, 64.6% for vildagliptin, and 92.4% for anagliptin, but not by saxagliptin (Figs. 5B, 5D, and 5F).

Hydrolysis of gliptin amide derivatives in recombinant DPPs. Fig. 6 shows that the amide derivatives were stable in buffers, but they could be hydrolyzed to carboxylic acid metabolites (including saxagliptin-amide) in DPP incubation system. Unlike in cases where gliptins were used as the substrates, the amide derivatives that hydrolyzed to carboxylic acid in DPP-2 were less than those in DPP-4, DPP-8, and FAP.

In Fig. 7, the formation rates of besigliptin-COOH from besigliptin and from besigliptin-amide were compared in DPP-4. Besigliptin-amide (100 μ M) could be hydrolyzed to carboxylic acid completely in 15 min. The formation rate from besigliptin-amide to the carboxylic acid (399 nmol/mg protein/min) was 3380-fold faster than that from besigliptin (0.118 nmol/mg protein/min). The consuming rate of amide into carboxylic acid (Fig. 8) was similar among besigliptin-amide (0.79), vildagliptin-amide (1.21), and saxagliptin-amide (1.76).

Distribution of DPP-2 and DPP-4 protein in the human/rat liver and kidney or corresponding subcellular organelles. Immunoblot analysis showed that the amount of DPP-2 in rat kidney was much higher than that in rat liver (Fig. 9A). Likely, the abundance of DPP-4 in rat kidney was also more than that in rat liver. However, the abundance of DPP-2 in human liver was comparable with that in the human kidney. Different from the distribution of DPP-2 in the human liver and kidney, the abundance of DPP-4 in the human kidney was higher than that in the human liver.

The subcellular localization of DPP-2 and DPP-4 in the liver and kidney was also detected (Fig. 9B). DPP-2 and DPP-4 were distributed in the mitochondria, microsomes, and cytosol in descending order in rat liver, human liver, and rat kidney.

Pharmacokinetics of besigliptin. The plasma concentration–time curves of besigliptin and its carboxylic acid metabolite after an oral administration of 3 mg/kg besigliptin to control and saxagliptin-treated rats are shown in Fig. 10. The AUC_{0-t} value for besigliptin in saxagliptin-treated rats was 21% higher than that of control rats. The AUC_{0-t} value for besigliptin-COOH in saxagliptin-treated rats was 20% lower than that of control rats.

The pharmacokinetic characters of besigliptin were also changed by AX8819, an inhibitor of

DPP-2 (Fig. 11). After an oral administration of AX8819, the AUC_{0-t} value for besigliptin was increased to 2.23-fold, and the AUC_{0-t} value for besigliptin-COOH was decreased to 62% compared with control rats.

Discussion

The nitrile group of cyanopyrrolidine DPP-4 inhibitors vildagliptin, anagliptin, and besigliptin could be hydrolyzed to the carboxylic acid, which were their major metabolites *in vivo*, accounting for 56.5% (He et al., 2009a), 29.2% (Furuta et al., 2013), and 31.6% (unpublished data) of the administered doses in humans, respectively. However, the nitrile group of saxagliptin could not be hydrolyzed. Thus, it is necessary to confirm the main enzymes involved in the formation of carboxylic acid metabolites of these cyanopyrrolidine DPP-4 inhibitors for proper combination of drugs to avoid drug–drug interaction. DPP-4 was reported to participate in the partial hydrolysis of vildagliptin (He et al., 2009a; Asakura et al., 2015) and anagliptin (Furuta et al., 2013). Asakura et al. demonstrated that DPP-4 is expressed in liver microsomes (Asakura et al., 2015). However, in the pre-study, we found that the carboxylic acid metabolites of gliptins could be also formed by the mitochondria and cytosol of liver and kidney. Therefore, we supposed that some other enzymes participated in the CN hydrolysis. At the same protein concentration, subcellular organelles of kidney produced more carboxylic acid metabolites than those of the liver, in rats and humans, indicating that the kidney is also an important organ for the hydrolytic metabolism of gliptins. The soluble form of DPP-4 was reported to also exist in the serum (Durinx et al., 2000). In Fig. 3, the hydrolysis of nitrile group in plasma was also observed, but much less than that in the liver and kidney, which would influence the detection accuracy of gliptins in the low plasma concentration. In our pre-study, the hydrolysis of besigliptin (5 μ M) in plasma could be inhibited by saxagliptin (100 μ M) by more than 90% (Supplemental Fig. S2), indicating that DPP-4 is the main participated isoform of hydrolysis in plasma. As a result, it is suggested that DPP-4 inhibitors are added to the plasma samples to avoid

hydrolysis by the DPP-4 in pharmacokinetic investigations of these cyanopyrrolidine DPP-4 inhibitors.

In DPP-4-knockout rats, the formation of vildagliptin carboxylic acid metabolite was only decreased by approximately 20% (He et al., 2009b). DPP-4 belongs to the serine peptidase family. Therefore, the hydrolysis activity of its homologous enzymes, including DPP-2, DPP-8, DPP-9, and FAP, to the nitrile group was also investigated. Besides DPP-4, DPP-2 showed the most turnover capacity of the hydrolytic metabolism of gliptins, followed by DPP-8, FAP, and DPP-9 (Figs. 4A–4C). Although the generation of carboxylic acid metabolites in DPP-4, DPP-8, DPP-9 and FAP was similar, it should not be neglected that the gliptins were all strong DPP-4 inhibitors. In this present study, a high concentration (100 μ M) of gliptins was used so that the amide concentration could be detected clearly. The high level of gliptins also inhibited the catalytic ability of DPP-4 powerfully. When 250 nM besigliptin was incubated in DPPs, only DPP-4 and DPP-2 showed a significant turnover ability of besigliptin to its carboxylic acid but no other DPPs (Supplemental Fig. S3). It was suggested that the affinity of gliptins to DPP-2 and DPP-4 was much greater than that to other DPPs. Lower concentration of gliptins preferred to enter the pocket of DPP-2 and DPP-4, whereas only much higher concentration of gliptins could get into the pocket of other DPPs. Considering the concentration of gliptins *in vivo* was not as high as 100 μ M, therefore, DPP-4 and DPP-2 were considered to have more contribution to the gliptin hydrolysis.

It was reported that the expression and activity of DPP-8 and DPP-9 are lower than those of DPP-4 in rats, monkeys and humans (Harstad et al., 2013; Fagerberg et al., 2014), combining with their limited hydrolysis ability, therefore, they were not chosen for the *in vitro* and *in vivo* inhibition

studies. Considering the stronger hydrolysis activity of DPP-2 and DPP-4 for both low and high concentration of gliptins, their protein expressions were determined in the liver and kidney subcellular organelles. Western blot results indicated that the expressions of DPP-2 and DPP-4 were higher in the mitochondria and microsomes of rat liver and kidney and human liver. In the cytosol, very low expressions of DPP-2 and DPP-4 (Fig. 9) were found, which also accorded with the hydrolytic activity results in the subcellular organelles (Fig. 3).

To further confirm the hydrolysis of gliptins catalyzed by DPP-4 and DPP-2, inhibition experiments were launched *in vitro* and *in vivo*. In the DPP-4 incubation system, the hydrolysis of besigliptin, vildagliptin, and anagliptin could be almost completely inhibited by the DPP-4 inhibitor, saxagliptin (Fig. 5). However, in the rats pretreated with saxagliptin, the AUC_{0-t} value of besigliptin-COOH was only decreased by 20%. In the DPP-2 incubation system with the physiological pH, the hydrolysis of three gliptins could be inhibited by DPP-2 inhibitor, AX8819 (Danilova et al., 2007). In the rats pretreated with AX8819, the AUC_{0-t} and C_{max} of besigliptin-COOH metabolite significantly decreased to 56.7% and 63.9%, respectively, whereas the AUC_{0-t} of the parent drug increased to 2.23-fold compared with the control rats. Using the docking method, we found that similar to DPP-4, besigliptin is located in the active triad of DPP-2 and bound to DPP-2 through hydrogen bonds to Glu-78, stabilizing the complex. By comparing the score between DPP-2 and DPP-4, we found that the score of DPP-2 for the metabolism of besigliptin is better than that of DPP-4, suggesting that the binding to DPP-2 is stronger (unpublished data). These results indicated that DPP-2 possibly made a greater contribution to the hydrolysis of gliptins than DPP-4. However, as the content of DPP-2 *in vivo* has not been confirmed so far, the contribution of DPP-2 needs further research.

In the incubation of besigliptin, vildagliptin, and anagliptin with DPPs, their corresponding amide metabolites could be detected (Fig. 4) and could also be detected in the human urine after an oral administration of besigliptin (Fig. 2). When the amide metabolite standards were incubated as substrates, a large amount of carboxylic acid metabolites were detected, with the most production in DPP-4, DPP-8, and FAP and the least in DPP-2 and DPP-9 incubation systems (Fig. 6). No carboxylic acid was detected in the buffer without enzymes. Unlike the case with amides as substrates, when the gliptins were used as substrates, carboxylic acid metabolites were generated mainly during DPP-2 incubation, but more amide metabolites were produced in DPP-8 incubation (Fig. 4). So it is supposed that there may be different hydrolysis metabolisms between DPP-2 and other DPPs. Surprisingly different from saxagliptin, the saxagliptin-amide could be hydrolyzed to carboxylic acid by DPPs (Fig. 6). In DPP-4 incubation, the formation rate from amide derivatives to carboxylic acid was much faster than that from gliptins to carboxylic acid (Figs. 7 and 8). These results indicated that DPP-4, DPP-2, and DPP-8 mainly participated in the CN hydrolysis of gliptins, and the formation of amide metabolites was the initial step of hydrolytic metabolism, which is also the rate-limiting step in generating the carboxylic end-products. Saxagliptin cannot be hydrolyzed to carboxylic acid possibly because its amide cannot be formed in the first step.

To test whether other compounds containing nitrile groups could also be hydrolyzed by DPP-4, lacosamide, finasteride, niclosamide, bicalutamide, and flutamide were incubated with DPP-4. None of them could be metabolized to amide or carboxylic acid metabolite (data not shown). The catalytic triad of human DPP-4 comprises Ser630, Asp708, and His740, which are located in a large cavity at the interface of the two domains of the protein (Thoma et al., 2003). To cyanopyrrolidine DPP-4

inhibitors, pyrrolidine was appended to an amino acid or the surrogate group to mimic proline, and the nitrile group was most likely covalently bound to Ser630 and within hydrogen bonding distance of Tyr547 (Oefner et al., 2003; Augeri et al., 2005). Thus, cyanopyrrolidine could bind to the active site of catalysis, providing the inhibitory activity and the potential of hydrolysis. Therefore, it is assumed that the precondition of the hydrolysis was that the nitrile group should enter the catalytic site of DPPs (Matteucci and Giampietro, 2009). The mechanism of nitrile group hydrolysis by DPP-4 was speculated (Fig. 12). The serine protease catalysis included the acylation of the active site serine, subsequent release of the amine leaving group, and hydrolysis of the acyl intermediate. The oxyanion of serine nucleophilic attacked nitrile carbon with the assistance from histidine. The electronegative nitrogen took the hydrogen of tyrosine and became imine. The first H₂O participated, and the imine was bound with a hydroxyl, which was so unstable that it transformed to the amide intermediate (Kim et al., 2006). The amide intermediate still positioned in the catalytic triad of Asp-His-Ser by hydrogen bonding and was also attacked by the oxyanion of serine to form a tetrahedral intermediate. The next step was the reconstruction of the carbonyl double bond with the expulsion of the leaving ammonia. The second molecule of water took part in the restoration of the carbonyl double bond, and finally, the catalytic triad was released to the beginning state. However, for DPP-2, the hydrolysis mechanism may be different because two molecules of water entered into the active site in one step. Therefore, the amide intermediate was hydrolyzed to the carboxylic acid more rapidly, so the number of carboxylic end-products was higher than that of the amide intermediate (Fig. 4).

In conclusion, this study found that besides DPP-4, cyanopyrrolidine gliptins could also be hydrolyzed to the amide metabolites and end-product carboxylic acid metabolites by other serine

peptidases in the DPP family, especially DPP-2. The effects of the above DPPs and their contribution of metabolism *in vivo* should be further evaluated. The study may also provide some useful information for drug design and metabolism investigation of nitrile-containing compounds.

Acknowledgments

We greatly appreciate Dr. Youhong Hu (Shanghai Institute of Materia Medica, Chinese Academy of Sciences) for the synthesis of AX8819 and Dr. Jingya Li (National Center for Drug Screening, Shanghai Institute of Materia Medica, Chinese Academy of Sciences) for kindly providing recombinant DPPs.

Authorship Contributions

Participated in research design: Kong, Pang, Chen.

Conducted experiments: Kong, Pang, Deng.

Contributed new reagents or analytic tools: Kong, Pang, Zhong, Chen.

Performed data analysis: Kong, Pang, Zhao, Zheng, Chen.

Wrote or contributed to the writing of the manuscript: Kong, Pang, Chen.

Conflicts of interest

The authors declare no conflicts of interest.

Reference

- Asakura M, Fujii H, Atsuda K, Itoh T, and Fujiwara R (2015) Dipeptidyl peptidase-4 greatly contributes to the hydrolysis of vildagliptin in human liver. *Drug Metab Dispos* **43**:477-484.
- Augeri DJ, Robl JA, Betebenner DA, Magnin DR, Khanna A, Robertson JG, Wang A, Simpkins LM, Taunk P, Huang Q, Han SP, Offei AB, Cap M, Xin L, Tao L, Tozzo E, Welzel GE, Egan DM, Marcinkeviciene J, Chang SY, Biller SA, Kirby MS, Parker RA, and Hamann LG (2005) Discovery and preclinical profile of Saxagliptin (BMS-477118): a highly potent, long-acting, orally active dipeptidyl peptidase IV inhibitor for the treatment of type 2 diabetes. *Journal of Medicinal Chemistry* **48**:5025-5037.
- Danilova O, Li B, Szardenings AK, Huber BT, and Rosenblum JS (2007) Synthesis and activity of a potent, specific azabicyclo[3.3.0]-octane-based DPP II inhibitor. *Bioorg Med Chem Lett* **17**:507-510.
- Durinx C, Lambeir AM, Bosmans E, Falmagne JB, Berghmans R, Haemers A, Schapé S, and De Meester I (2000) Molecular characterization of dipeptidyl peptidase activity in serum. *Eur J Biochem* **267**:5608-5613.
- Fagerberg L, Hallstrom BM, Oksvold P, Kampf C, Djureinovic D, Odeberg J, Habuka M, Tahmasebpour S, Danielsson A, Edlund K, Asplund A, Sjostedt E, Lundberg E, Szigartyo CA, Skogs M, Takanen JO, Berling H, Tegel H, Mulder J, Nilsson P, Schwenk JM, Lindskog C, Danielsson F, Mardinoglu A, Sivertsson A, von Feilitzen K, Forsberg M, Zwahlen M, Olsson I, Navani S, Huss M, Nielsen J, Ponten F, and Uhlen M (2014) Analysis of the human tissue-specific expression by genome-wide integration of transcriptomics and antibody-based proteomics. *Mol Cell Proteomics* **13**:397-406.

Fleming FF, Yao L, Ravikumar PC, Funk L, and Shook BC (2010) Nitrile-containing pharmaceuticals: efficacious roles of the nitrile pharmacophore. *J Med Chem* **53**:7902-7917.

Furuta S, Smart C, Hackett A, Benning R, and Warrington S (2013) Pharmacokinetics and metabolism of [14C]anagliptin, a novel dipeptidyl peptidase-4 inhibitor, in humans. *Xenobiotica* **43**:432-442.

Gautier JF, Fetita S, Sobngwi E, and Salaün-Martin C (2005) Biological actions of the incretins GIP and GLP-1 and therapeutic perspectives in patients with type 2 diabetes. *Diabetes Metab* **31**:233-242.

Harstad EB, Rosenblum JS, Gorrell MD, Achanzar WE, Minimo L, Wu J, Rosini-Marthaler L, Gullo R, Ordway ND, Kirby MS, Chadwick KD, Cosma GN, and Moyer CF (2013) DPP8 and DPP9 expression in cynomolgus monkey and Sprague Dawley rat tissues. *Regul Pept* **186**:26-35.

He H, Tran P, Yin H, Smith H, Batard Y, Wang L, Einolf H, Gu H, Mangold JB, Fischer V, and Howard D (2009a) Absorption, metabolism, and excretion of [14C]vildagliptin, a novel dipeptidyl peptidase 4 inhibitor, in humans. *Drug Metab Dispos* **37**:536-544.

He H, Tran P, Yin H, Smith H, Flood D, Kramp R, Filipeck R, Fischer V, and Howard D (2009b) Disposition of vildagliptin, a novel dipeptidyl peptidase 4 inhibitor, in rats and dogs. *Drug Metab Dispos* **37**:545-554.

Kim YB, Kopcho LM, Kirby MS, Hamann LG, Weigelt CA, Metzler WJ, and Marcinkeviciene J (2006) Mechanism of Gly-Pro-pNA cleavage catalyzed by dipeptidyl peptidase-IV and its inhibition by saxagliptin (BMS-477118). *Arch Biochem Biophys* **445**:9-18.

Matteucci E and Giampietro O (2009) Dipeptidyl peptidase-4 (CD26): knowing the function before

inhibiting the enzyme. *Curr Med Chem* **16**:2943-2951.

Oefner C, D'Arcy A, Mac Sweeney A, Pierau S, Gardiner R, and Dale GE (2003) High-resolution structure of human apo dipeptidyl peptidase IV/CD26 and its complex with 1-[(2-[(5-iodopyridin-2-yl)amino]-ethyl)amino)-acetyl]-2-cyano-(S)-pyrrolidine. *Acta Crystallogr D Biol Crystallogr* **59**:1206-1212.

Su H, Boulton DW, Barros A, Wang L, Cao K, Bonacorsi SJ, Lyer RA, Humphreys G, and Christopher LJ (2012) Characterization of the in vitro and in vivo metabolism and disposition and cytochrome P450 inhibition/induction profile of saxagliptin in human. *Drug Metabolism and Disposition* **40**:1345-1356.

Thoma R, Löffler B, Stihle M, Huber W, Ruf A, and Hennig M (2003) Structural Basis of Proline-Specific Exopeptidase Activity as Observed in Human Dipeptidyl Peptidase-IV. *Structure* **11**:947-959.

Footnotes

Fandi Kong and Xiaoyan Pang contributed equally to this work.

This research was financially supported by the National Natural Science Foundation of China [81573500] and the Strategic Priority Research Program of the Chinese Academy of Sciences [XDA 12050306].

Figure Legends:

Fig. 1. Structures of typical cyanopyrrolidine DPP-4 inhibitors.

Fig. 2. Extracted ion chromatograms of metabolites in human plasma sample 2 h post-dose (A) and 0–24 h urine sample (B) after 100 mg oral dose of besigliptin.

Fig. 3. Hydrolysis of vildagliptin (0.50 μ M) (A and B), besigliptin (0.25 μ M) (C and D), and anagliptin (E and F) in subcellular organelles of rat liver and kidney and human liver ($n = 3$).

Fig. 4. Hydrolysis of besigliptin (A), vildagliptin (B), anagliptin (C), and saxagliptin (D) in DPP-4, DPP-2, DPP-8, DPP-9, FAP, and their corresponding incubation buffer. Data are displayed as the mean of two separate samples.

Fig. 5. Hydrolysis of besigliptin (10 μ M) (A: DPP-4; B: DPP-2), vildagliptin (10 μ M) (C: DPP-4; D: DPP-2), anagliptin (10 μ M) (E: DPP-4; F: DPP-2) in the presence or absence of saxagliptin (50 μ M) or AX8819 (50 μ M) ($n = 3$) in PBS (pH 7.4). ***, $p < 0.001$ compared with control.

Fig. 6. Hydrolysis of besigliptin-amide (A), vildagliptin-amide (B), and saxagliptin-amide (C) in DPP-4, DPP-2, DPP-8, DPP-9, FAP, and their corresponding incubation buffer. Data are displayed as the mean of two separate samples.

Fig. 7. Formation rate of besigliptin-COOH from besigliptin (100 μ M) (A) and besigliptin-amide (100 μ M) (B) in DPP-4 incubation system ($n = 3$).

Fig. 8. Formation rate from besigliptin-amide (k_B), vildagliptin-amide (k_V), and saxagliptin-amide (k_S) to their corresponding carboxylic acid ($n = 3$).

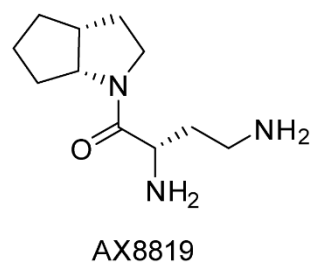
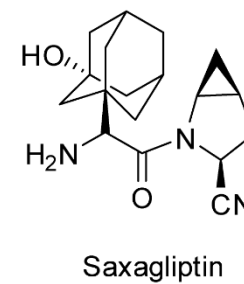
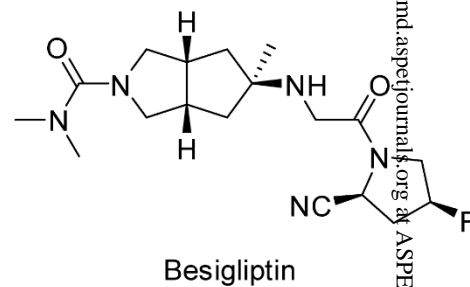
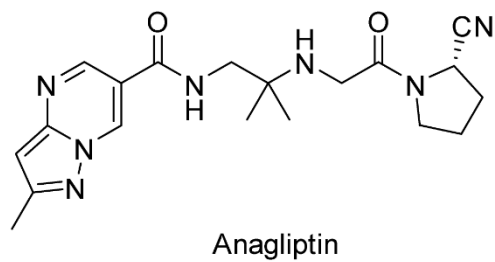
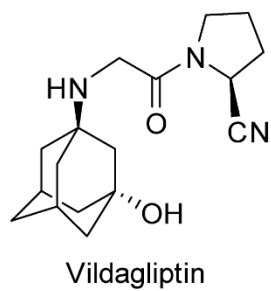
Fig. 9. Immunoblot analysis of DPP-2 and DPP-4 in the rat or human liver and kidney homogenates (A) or corresponding subcellular organelles (B). Homogenates or different intracellular fractions

were subjected to 4% – 20% Bis-Tris polyacrylamide gel and probed with anti-DPP-2 or anti-DPP-4 antibody.

Fig. 10. Mean plasma concentration-time profiles of besigliptin (A) and its carboxylic acid metabolite (B) following an oral administration of besigliptin (3 mg/kg) to control and saxagliptin-treated rats.

Fig. 11. Mean plasma concentration-time profiles of besigliptin (A) and its carboxylic acid metabolite (B) following an oral administration of besigliptin (1 mg/kg) to control and AX8819-treated rats.

Fig. 12. Hydrolysis mechanism of nitrile group by the catalytic triad of Asp-His-Ser with the amide intermediate.

**Fig.1**

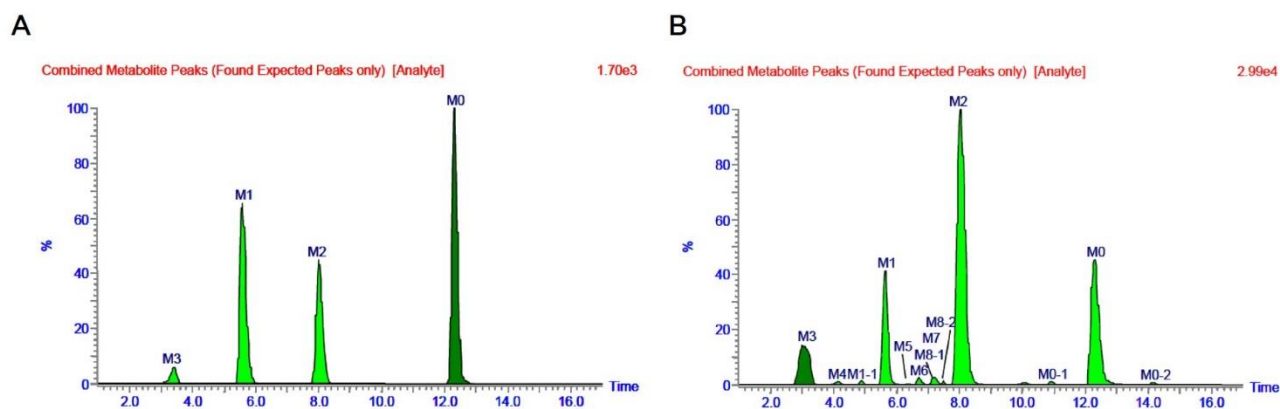


Fig. 2

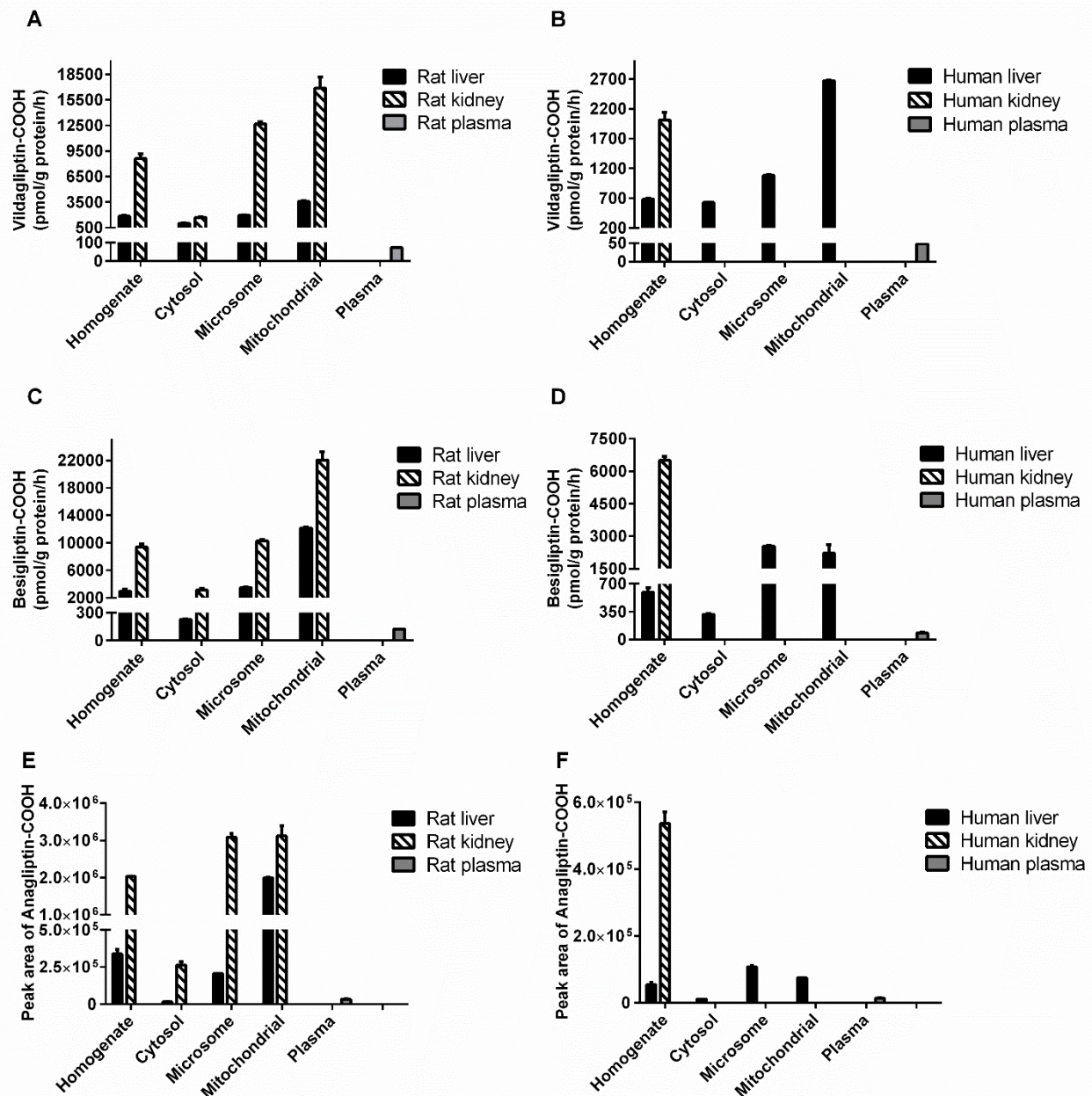


Fig. 3

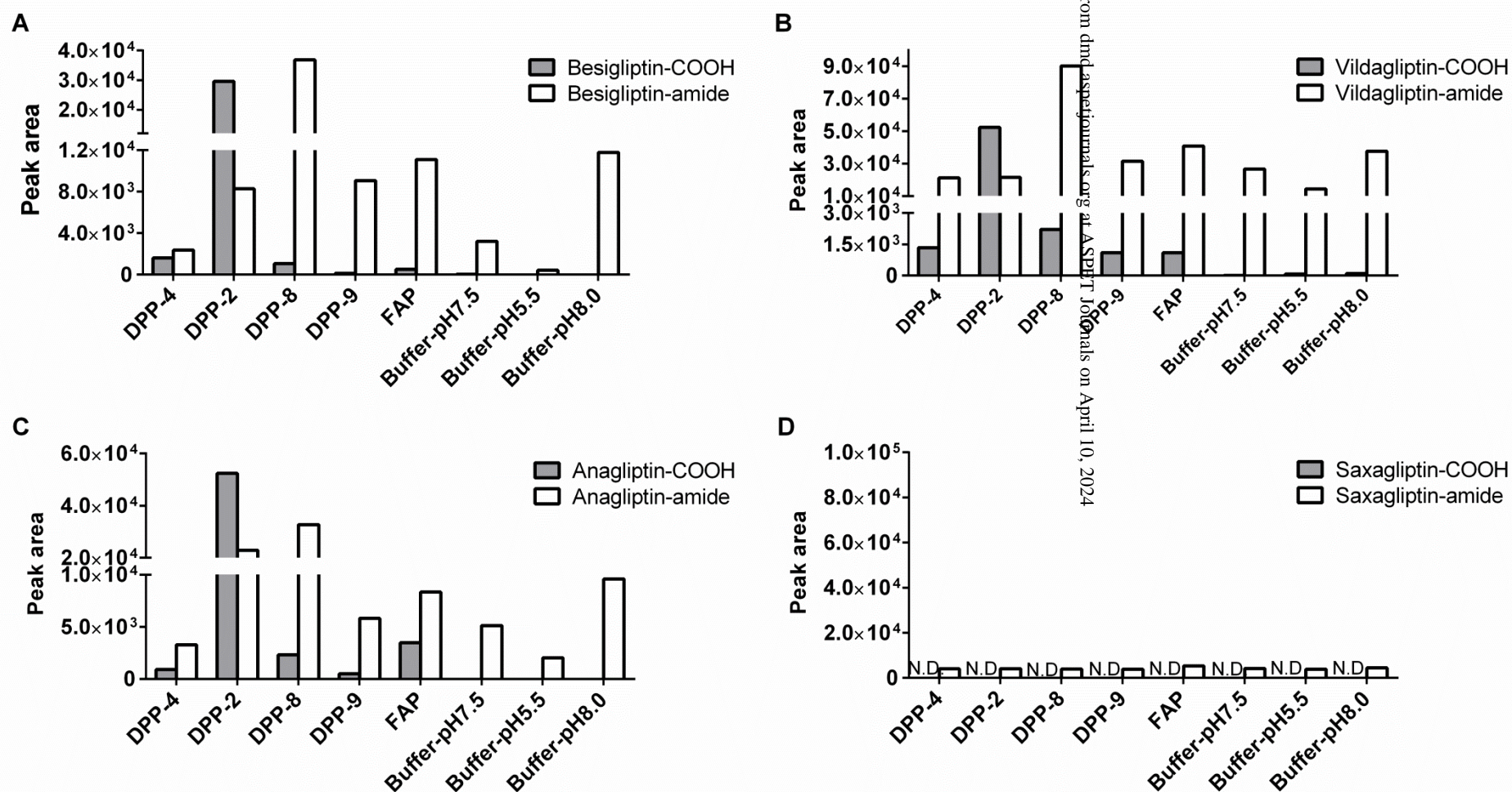


Fig. 4

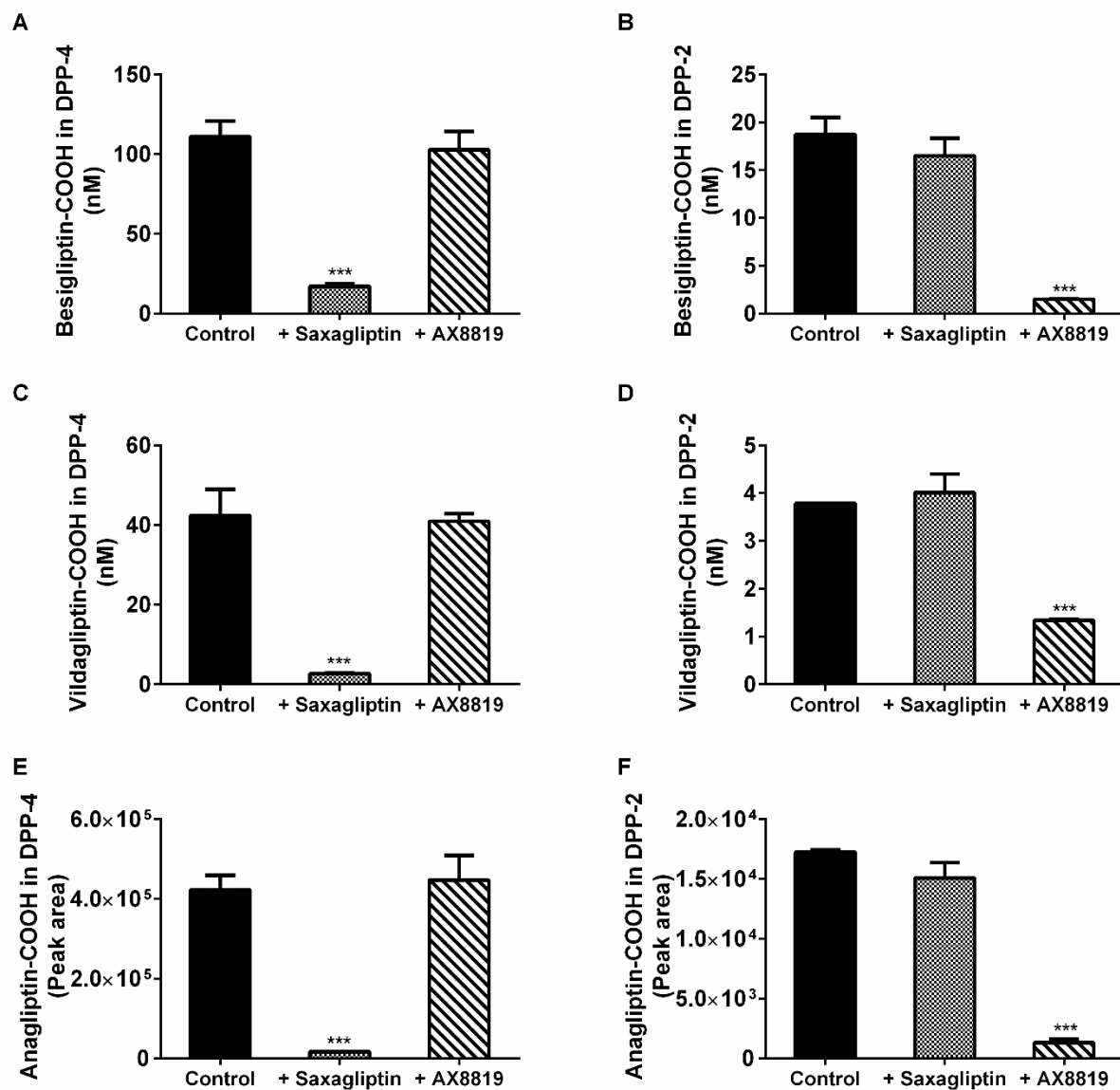


Fig. 5

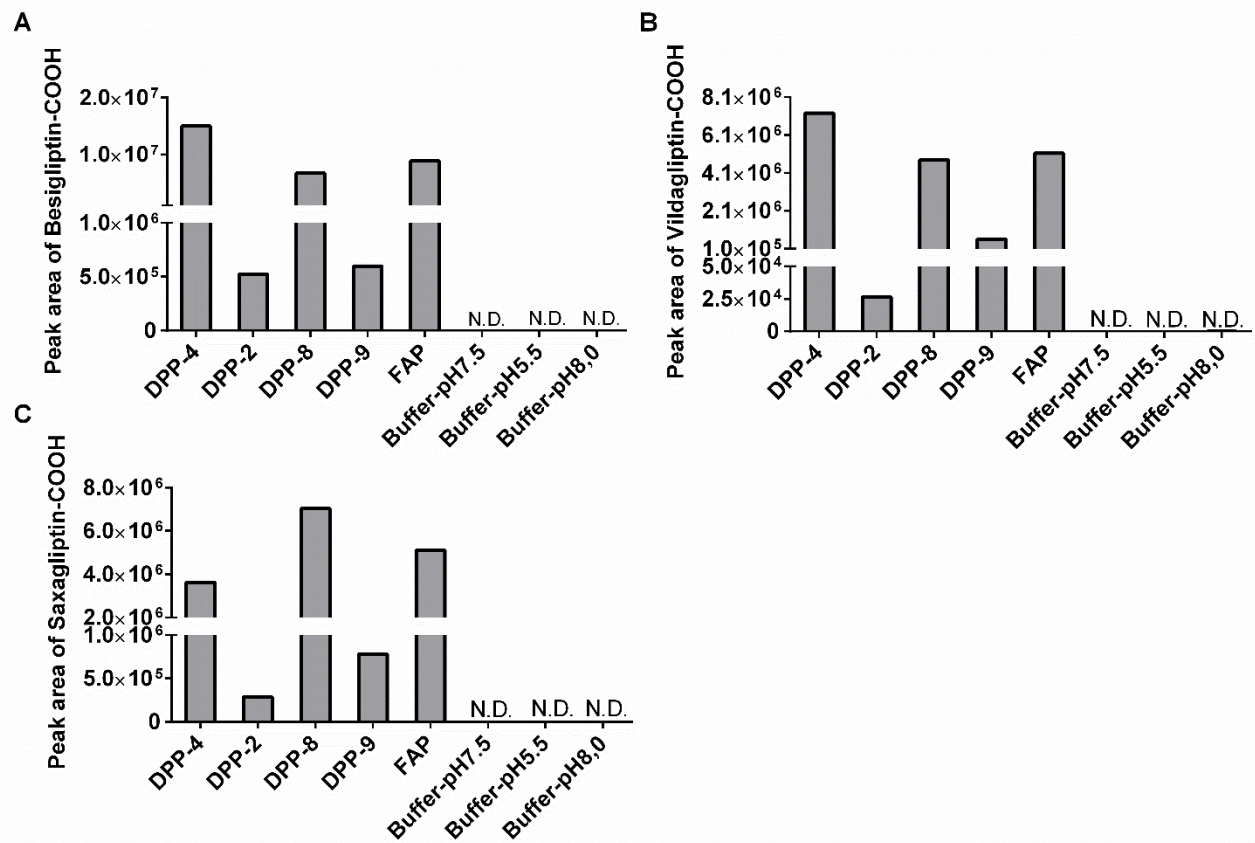


Fig. 6

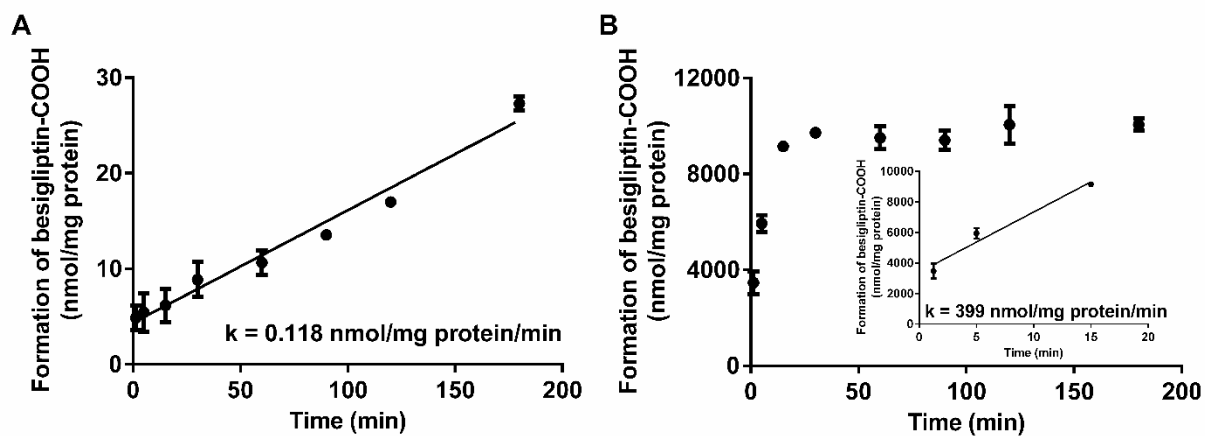


Fig. 7

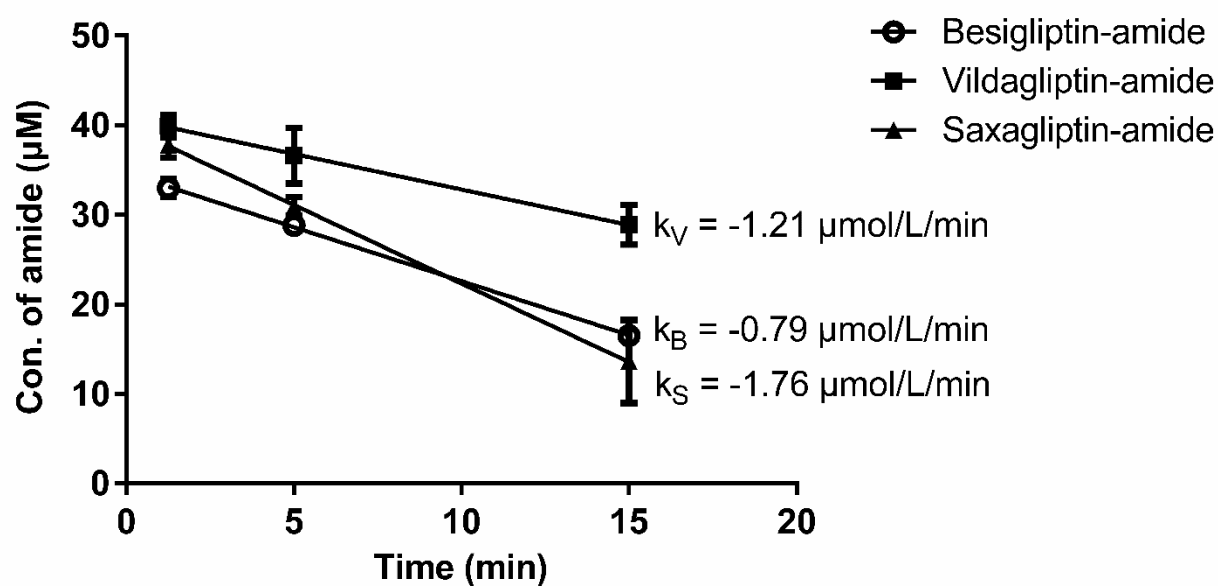


Fig. 8

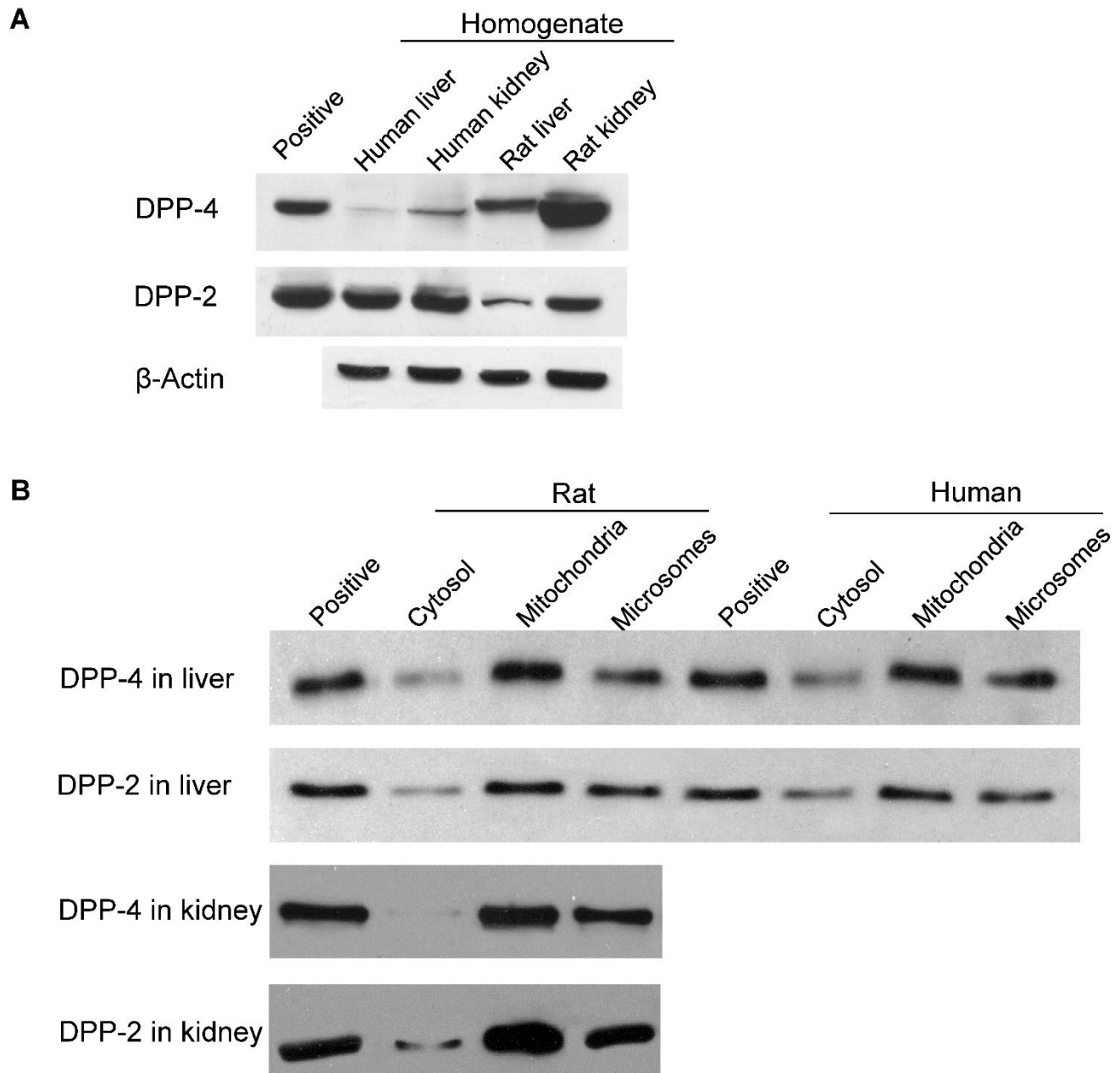


Fig. 9

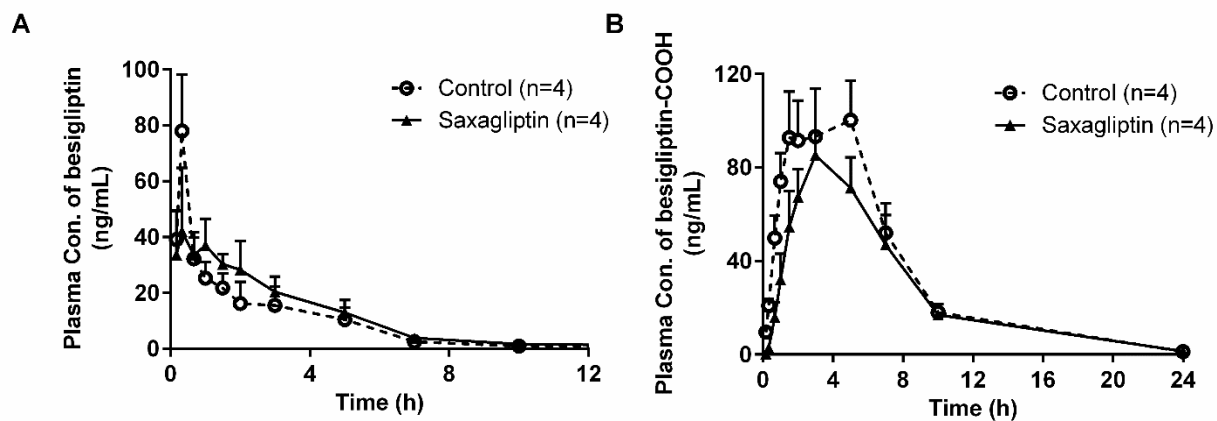


Fig. 10

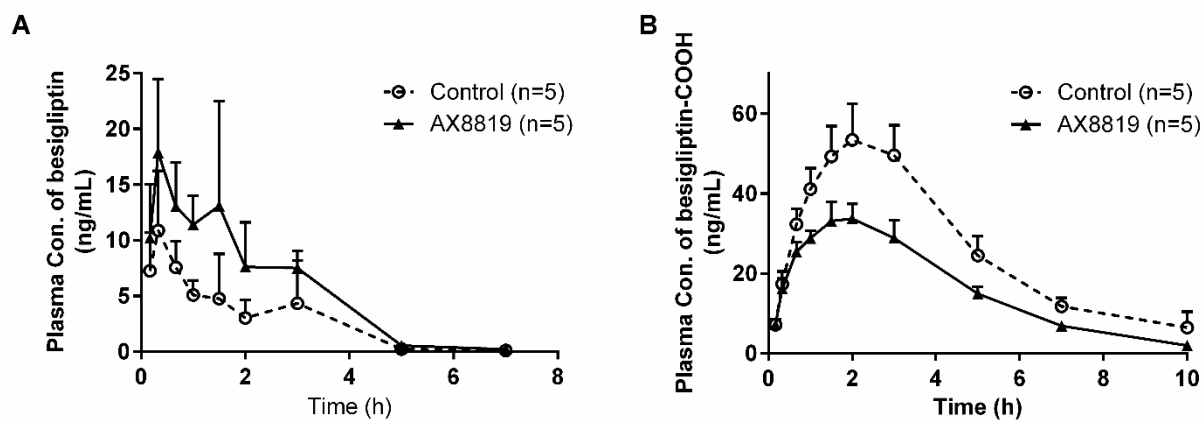


Fig. 11

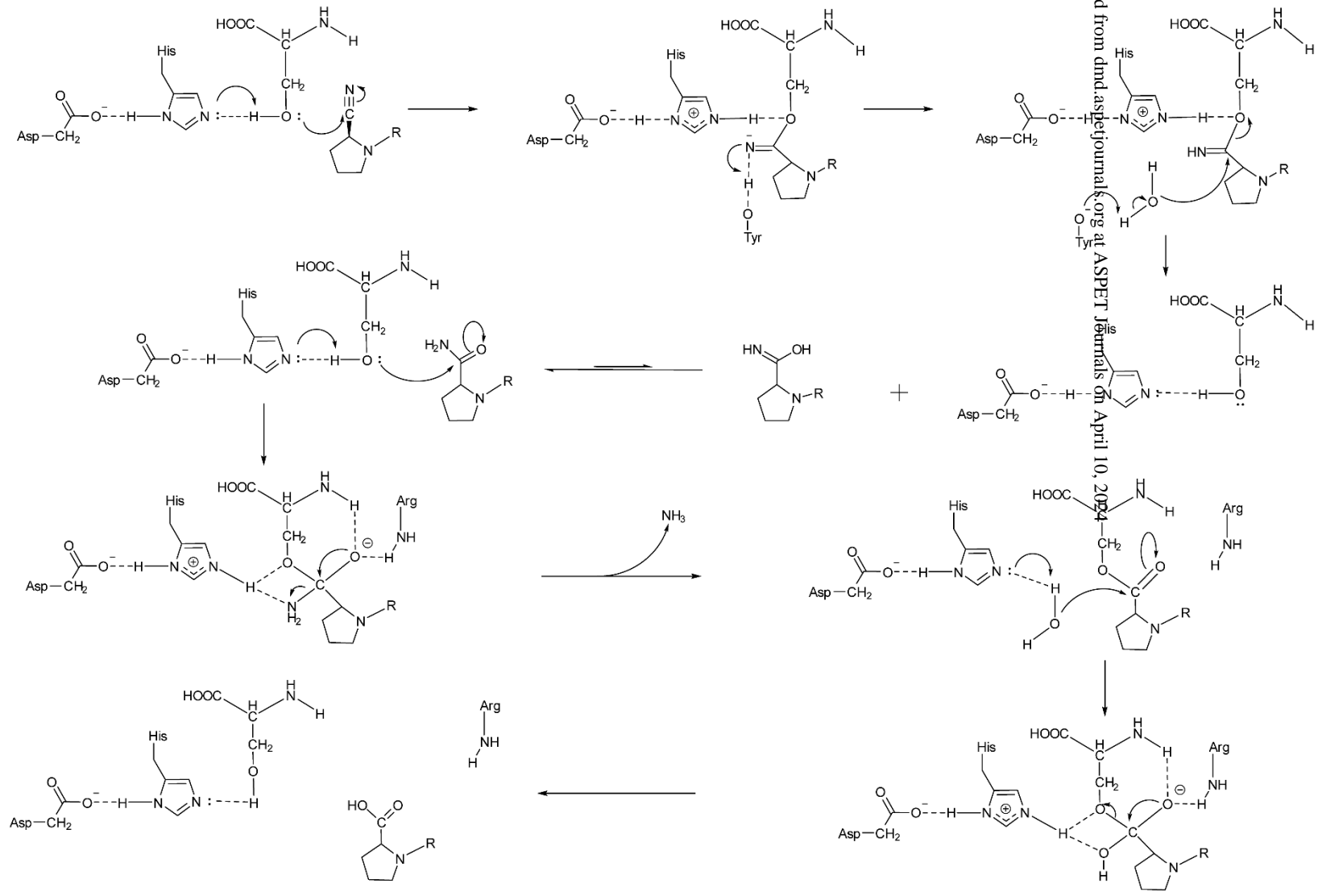


Fig. 12